# Anti-proliferation effects of trifolirhizin on MKN45 cells and possible mechanism

XINGANG LU[1*], JIANXIA MA[2*], HONGFU QIU[1], LIU YANG[3], LEI CAO[4] and JIE SHEN[5]

Departments of [1]Traditional Chinese Medicine and [2]Gastroenterology, Huadong Hospital, Fudan University, Shanghai 200040; [3]Department of Oncology, Baoshan Hospital of Integrated Traditional Chinese and Western Medicine, Shanghai University of Traditional Chinese Medicine, Shanghai 201999; [4]Department of Nursing, The 19th Ward, Longhua Hospital, Shanghai University of Traditional Chinese Medicine, Shanghai 200032; [5]Department of Pharmacy, Huadong Hospital, Fudan University, Shanghai 200040, P.R. China

Received May 11, 2016; Accepted September 6, 2016

DOI: 10.3892/or.2016.5125

**Abstract.** Trifolirhizin is a compound isolated from *Sophora flavescens*. It has been shown to exert cytotoxicity on several cancer cell lines. However, the underlying mechanism remains unknown. MKN45 cells were used as a research model. We assessed the cytotoxicity of trifolirhizin to MKN45 by MTT. Hoechst staining and TUNEL method were used to demonstrate apoptosis. Flow cytometry was used to determine cell cycle and ratio of apoptosis. Caspase activity assay was used to examine the activation of caspase cascade pathways. Western blotting was used to explore the protein levels. Consistently, trifolirhizin inhibited MKN45 xenograft tumor growth *in vivo*. Trifolirhizin caused a significantly decreased proliferation of MKN45 cells in a time- and dose-dependent manner, with $IC_{50}$ values of 33.27±2.06 $\mu$g/ml at 48 h. Western blot assay manifested that trifolirhizin activated the EGFR-MAPK signaling pathways. This study indicated that trifolirhizin may be a therapeutic application in human gastric cancer therapy.

## Introduction

Gastric cancer is one of prevailing cancers worldwide accounting for nearly 8-10% of cancer mortality (1). According to published reports, there are approximately one million gastric cancer cases with 73,800 deaths in 2008 (2). In recent years, many advances have taken place in diagnosis and treatment (3). However, the mortality of gastric cancer remains 70% especially with late stage patients (4). Pharmacotherapy remains the effective strategy for treatment of gastric cancer (5). Screening effective agents from herb plants have been proved efficient (6). Many constituent have been demonstrated with antitumor effects both *in vitro* and *in vivo*, for instance: celastrol (7), bigelovin (8), and parthenolide (9). Other natural compounds also demonstrated many functions leading to cell proliferation, cell differentiation, apoptosis and cell cycle changes (10,11).

*Sophora flavescens* have been widely planted in East Asian countries as herbal plants and cosmetics (12). The root of *Sophora flavescens* was frequently used for treatment of mental health, inflammation, asthmas, and microbial activities (13-15). Trifolirhizin is a natural pterocarcan flavonoid extracted from *Sophora flavescens* (16). Published reports demonstrated its chemical structure (Fig. 1A) (17). Trifolirhizin has many pharmacological activities, such as hepatoprotective (18), anti-inflammatory (19), anti-proliferation (20), and skin-whitening (21). Trifolirhizin is also a biologically active constituent of Zeng-Sheng-Ping, a commercial Chinese traditional medicine for cancer prevention (22). Accumulating reports manifested that trifolirhizin had anti-proliferative activities in melanoma B16 cells, human A2780 ovarian and H23 lung cancer cells *in vitro* (19,21). Trifolirhizin also induced apoptosis in human leukemia HL-60 cells *in vitro* (23). Despite reports on the trifolirhizin cytotoxicity effect on various cells, the intrinsic mechanism of cytotoxicity and apoptosis triggered by trifolirhizin remains unknown. Herein, it is demonstrated that trifolirhizin induce apoptosis and cell cycle arrest while we explored also the mechanism of activation.

## Materials and methods

*Reagents and trifolirhizin preparation*. Trifolirhizin standard preparation (purity >98%) were purchased from Chinese National Institute for the Control of Pharmaceutical and Biological Products (Beijing, China). All other chemicals used were provided from Sigma-Aldrich (St. Louis, MQ, USA). Trifolirhizin was dissolved in DMSO. Cells were treated with increasing concentrations of trifolirhizin for designated hours. Control groups were exposed to the same volumes of DMSO under the same conditions.

*Correspondence to:* Dr Jie Shen, Department of Pharmacy, Huadong Hospital, Fudan University, 221 West YanAn Road, Shanghai 200040, P.R. China
E-mail: shj421@126.com

*Contributed equally

*Key words:* human gastric cancer MKN45 cells, apoptosis, cell cycle arrest, trifolirhizin, EGFR-MAPK

*Cell culture and cell viability assay*. MKN45, L02, HEK293 cells were purchased from the Cell Bank of Chinese Academy of Sciences (Shanghai, China). All cells were maintained in RPMI-1640 medium (Gibco, Carlsbad, CA, USA) with 10% fetal calf serum (Gibco) containing antibiotics (100 IU/ml penicillin and 100 IU/ml streptomycin) at 37˚C in an atmosphere containing 5% $CO_2$. The 3 types of cell lines were treated with various concentrations of trifolirhizin for suitable times. Cell viability of control and experiment cells were investigated using the 3-(4, 5-dimethylthiazol-2-yl)-2, 5-diphenyl-2H-tetrazolium bromide (MTT) assay. The absorbance at 570 nm was assessed using a microplate reader (Perkin-Elmer Inc., Waltham, MA, USA).

*Apoptosis detection of Hoechst 33342 staining and TUNEL staining*. MKN45 cells ($10^5$) were cultured on cover-slide and treated as described above. For Hoechst 33342 staining, cells were added with Hoechst 33342 (5 $\mu$g/ml) at 4˚C for 10 min in the dark (Beyotime, Haimeng, China). For terminal deoxynucleotidyl transferase (TdT)-mediated dUTP nick end labeling (TUNEL) staining (Roche, Basel, Switzerland), TUNEL kit was used to analyze cell DNA fragmentation in apoptotic cells according to the manufacturer's instructions. Trifolirhizin-treated cells after fixing was added by moderate TUNEL and DAPI (Beyotime). Finally, apoptotic cells were observed using an inverted fluorescence microscope (D5100, Nicon, Tokyo, Japan).

*Flow cytometry assay for ratio of apoptosis*. MKN45 cell ($2\text{-}5x10^5$) apoptosis quantification was analyzed according to the Annexin V&PI kit manufacturer's instructions (Selleck Chemicals, Houston, TX, USA). A minimum of $10^5$ trifolirhizin-treated cells were counted for each detection and immediately assessed by FACSCalibur flow cytometry (BD Biosciences, San Jose, CA, USA). Final sample data were reported as percentage of apoptotic cells (sum of early-phase apoptosis at right down quadrant and late-apoptosis at right upper quadrant).

*Assay of mitochondrial membrane potential (MMP)*. The JC-10 assay kit (AAT Bioquest, CA, USA) was used to assess the change tendency in mitochondrial membrane potential (MMP). The kit was applied according to the manufacturer's instructions. MKN45 cells were incubated in 96-well plate and exposed to trifolirhizin under desired concentrations. JC-10 working solutions (50 $\mu$l) were added into each well. After incubation and re-suspending in buffer B, the treated and control MKN45 cell suspensions were measured with an excitation filter of 490 nm while emission filter of 525 nm (green) and another excitation filter of 490 nm while emission filter of 590 nm (red) by a microplate reader (Perkin-Elmer).

*Cell cycle assay*. PI was employed for cycle analysis (Beyotime). After trifolirhizin treatment at 48 h, MKN45 carcinoma cells were harvested from 6-cm culture plates and subsequently fixed with 70% pre-cooled ethanol. After washing and centrifufation, cell pellets were re-suspended in staining solutions containing RNase A (10 $\mu$g/ml) with PI (5 $\mu$g/ml) under darkness. Cells treated with trifolirhizin and control were incubated for 30 min and then tested with a FACSCalibur cytometer system (BD Biosciences). Cell cycles were measured using ModFit LT3.2 software.

*Western blot analysis*. Western blotting was used to investigate the levels of apoptotic and related signaling pathway proteins. Concisely, cells treated with trifolirhizin and control were lysed with lysis buffer (Beyotime) and centrifuged. Cell proteins were fractionated by 8-12% SDS-PAGE. The proteins were electro-transferred onto the nitrocellulose membranes, using the BCA kit to adjust protein levels (Beyotime). The proteins levels were assessed using primary antibody, including Bcl-2, Bax, PARP, c-Myc, caspase-3, caspase-9, p-JNK, p-ERK, p-P38, JNK, P38, ERK, P53, β-actin (CST, Beverly, MA, USA), followed by incubation with anti-mouse/rat HRP-labeled secondary antibodies. The β-actin antibody was performed as control. The signals were invested by ECL chemiluminescence (BD Biosciences). The tendency of increasing or decreasing of proteins levels were analyzed comparing to control.

*Animals*. The animal study was licensed by the Institutional Animal Care and Use Committee of Fudan University and performed strictly accordance with the Declaration of Helsinki and the Guide for the Care and the Use of Laboratory Animals. The 6-week-old BALB/C nude mice were obtained from Shanghai Slac Laboratory Animal Corporation and maintained in a sterile humidified environment with average temperature at 22˚C. The mice were divided into 4 groups: 1 control group and 3 treatment groups (N=6) with increasing trifolirhizin. MKN45 cells were harvested, diluted to desired concentrations ($5x10^6$) and injected intraperitoneally into the right flank of each mouse. Then, trifolirhizin was injected into the BALB/C nude mice when tumor volume achieved a mean group size of 100 $mm^3$. The saline was injected into control group. All mouse groups were injected every 3 days. BALB-nu mice were sacrificed at 24 h when tumor volume achieved average group size of 1,000 $mm^3$. MKN45 tumor xenografts were evaluated and fixed for further experiments. Tumor volumes were evaluated as ($W^2$ x L)/2 per 3 days using micrometer calipers, and tumor weights were calculated.

*Immunohistochemistry*. The xenografted MKN45 tumor tissue samples were removed and cut to desired small pieces. samples (5 $\mu$m) were fixed and stained by cleaved-caspase-3 and Ki67 antibodies, respectively, for immunohistochemistry. We observed the visual images using an inverted fluorescence microscope (D5100, Nicon). The immunohistochemistry positive cells were counted and analyzed using ImageJ Pro 6.0 (National Institutes of Health).

*Statistical analysis*. We performed triplicate experiments using independent samples. Results were expressed as mean values ± standard deviation (mean ± SD). Statistical significance of our present results was determined using the one-way ANOVA. All statistical analyses were performed with commercial SPSS software (SPSS19.0, Chicago, IL, USA).

## Results

*Trifolirhizin exerts anti-proliferation effects in human gastric cancer cells*. Published reports have manifested that trifoli-

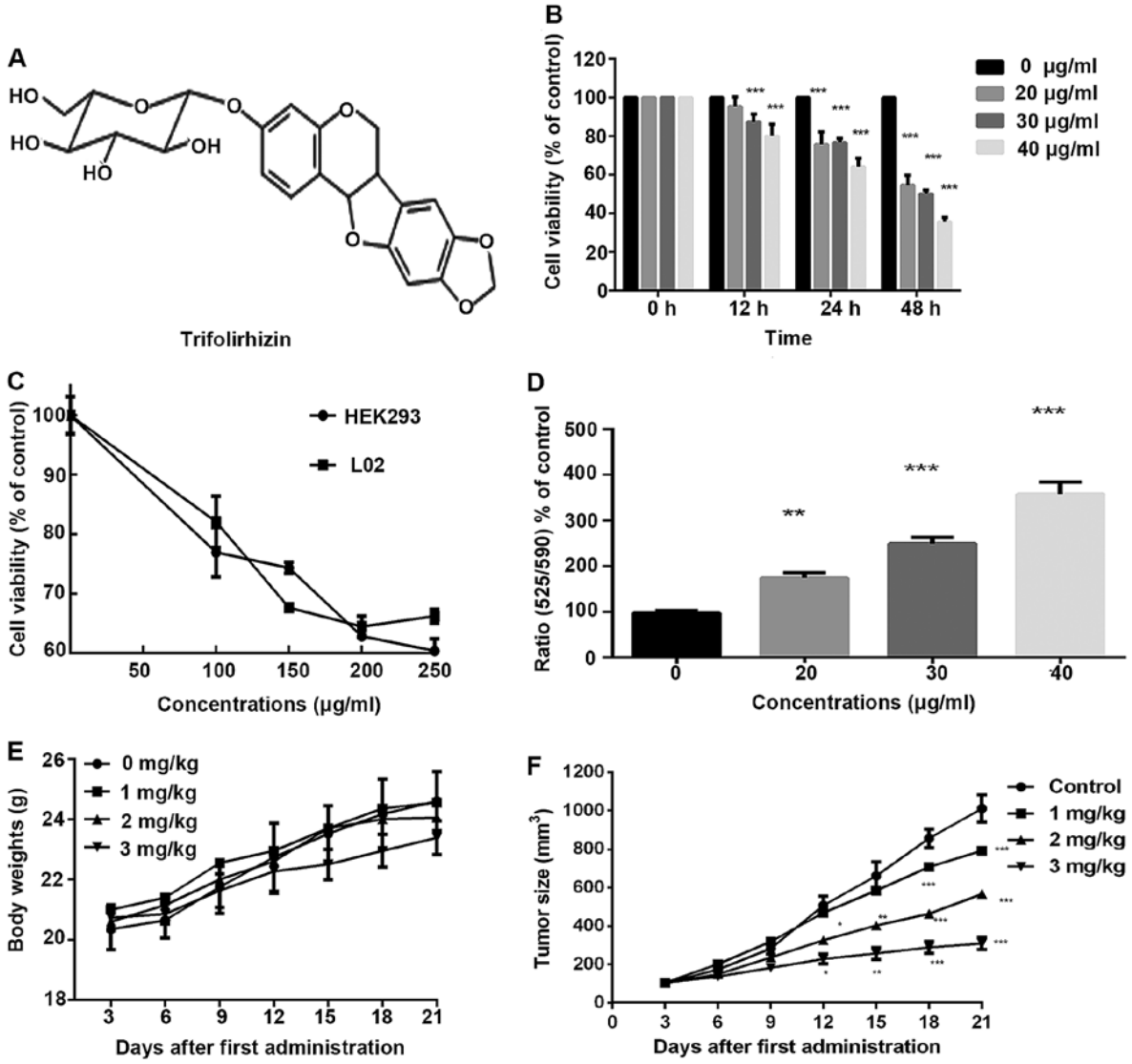


Figure 1. The inhibition effect of trifolirhizin on different cells. Cells were exposure for 48 h with increasing trifolirhizin or combined with EGF. (A) The chemical structure of trifolirhizin. (B) MTT assay of MKN45 cells treated with increasing trifolirhizin for 48 h. (C) Effect of trifolirhizin on normal HEK293 and L02 cells using MTT assay for 48 h. (D) Collapse of MMP in MKN45 cells induced with trifolirhizin for 24 h. (E) The body weights of BALB-nu MKN45 model. (F) The suppressed tumor growth effect of trifolirhizin in MKN45 BALB-nu models. Statistical differences were compared between trifolirhizin treatment group vs. control group at the levels of $^{*}P<0.05$, $^{**}P<0.01$ or $^{***}P<0.001$.

rhizin is cytotoxic on cancer cells. MTT assay was used to assess the numbers of viable MKN45 cells. Exposure under trifolirhizin results in a concentration- and time-dependent suppression of MKN45 cell viability (Fig. 1B). The trifolirhizin exposure time was 48 h in the present examination. The $IC_{50}$ value of trifolirhizin on MKN45 cells was 33.27±2.06 μg/ml. We also conducted MTT assay to evaluate the efficacy of trifolirhizin on a human normal liver cell line and human normal kidney cell line *in vitro*. To our satisfaction, >60% tested cells were viable when treated with increasing trifolirhizin dose ≤250 μg/ml. The apparently higher $IC_{50}$ value of trifolirhizin on two normal human cell lines exhibited more safety and further implication possibility (Fig. 1C).

*Trifolirhizin induces apoptosis in human stomach cancer cells in vitro*. MKN45 cells were treated with desired concentrations of trifolirhizin as above at 48 h. Hoechst staining exhibited visual images with cell shrinkage, nuclear fragmentation and chromatin compaction of apoptosis (Fig. 4A). Images indicated that trifolirhizin lead to increasing population of apoptotic cells. Consistently, TUNEL staining showed a significant difference between trifolirhizin treated cells vs. the vehicle control, the ratio of green staining (apoptotic) vs blue staining (normal) arise with increasing trifolirhizin (20-40 μg/ml, shown in Fig. 4B). Annexin V/PI assay was performed to evaluate the apoptotic population quantitation after trifolirhizin exposure. In this study, trifolirhizin significantly triggered apoptosis. The apoptotic population in trifolirhizin (20-40 μg/ml) induced MKN45 cells increased (Fig. 2). The JC-10 assay was used to indicate the mitochondrial outer membrane permeabilization after trifolirhizin treatment in early phase. Fig. 1D demonstrated that red fluorescence (normal cells) was decreased while green fluorescence (apoptotic cells) increased with trifolirhizin treatment (20-40 μg/ml) at 24 h, so the

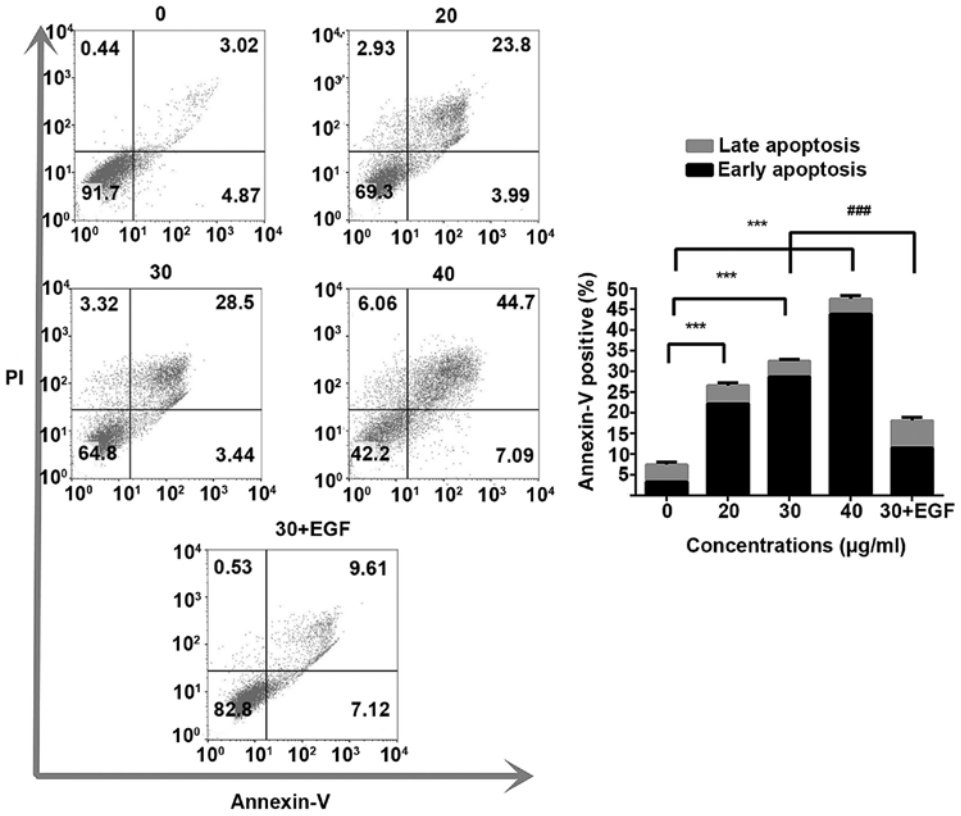


Figure 2. Trifolirhizin induced apoptosis in MKN45 cells. Cells were induced with increasing trifolirhizin or combined with EGF for 48 h. Flow cytometry analyses were used to assess the apoptosis of MKN45 cells with multiple dose of trifolirhizin treatment or combined with EGF for 48 h. Statistical differences between trifolirhizin treatment group vs. control group were considered significant at the levels of $^{*}$P<0.05, $^{**}$P<0.01 or $^{***}$P<0.001. Statistical differences between trifolirhizin treatment group vs. combination group were considered significant at the levels of $^{\#}$P<0.05, $^{\#\#}$P<0.01, $^{\#\#\#}$P<0.001.

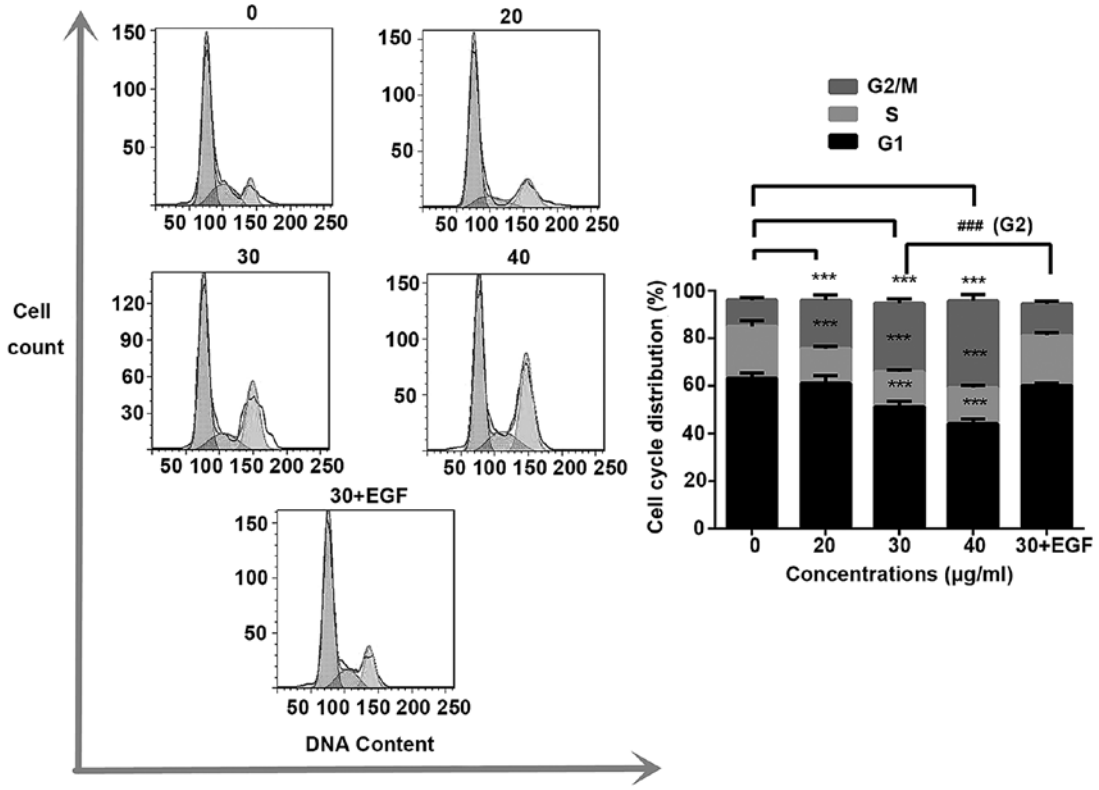


Figure 3. Trifolirhizin induced cell cycle arrest in MKN45 cells. Cells were treated with increasing trifolirhizin or combined with EGF for 48 h. Flow cytometry analyses were used to evaluate the cell cycle distributions of MKN45 cells with trifolirhizin treatment or combined with EGF for 48 h. Statistical differences between trifolirhizin treatment group vs. control group were considered significant at the levels of $^{*}$P<0.05, $^{**}$P<0.01 or $^{***}$P<0.001. Statistical differences between trifolirhizin treatment group vs. combination group were considered significant at the levels of $^{\#}$P<0.05, $^{\#\#}$P<0.01, $^{\#\#\#}$P<0.001.

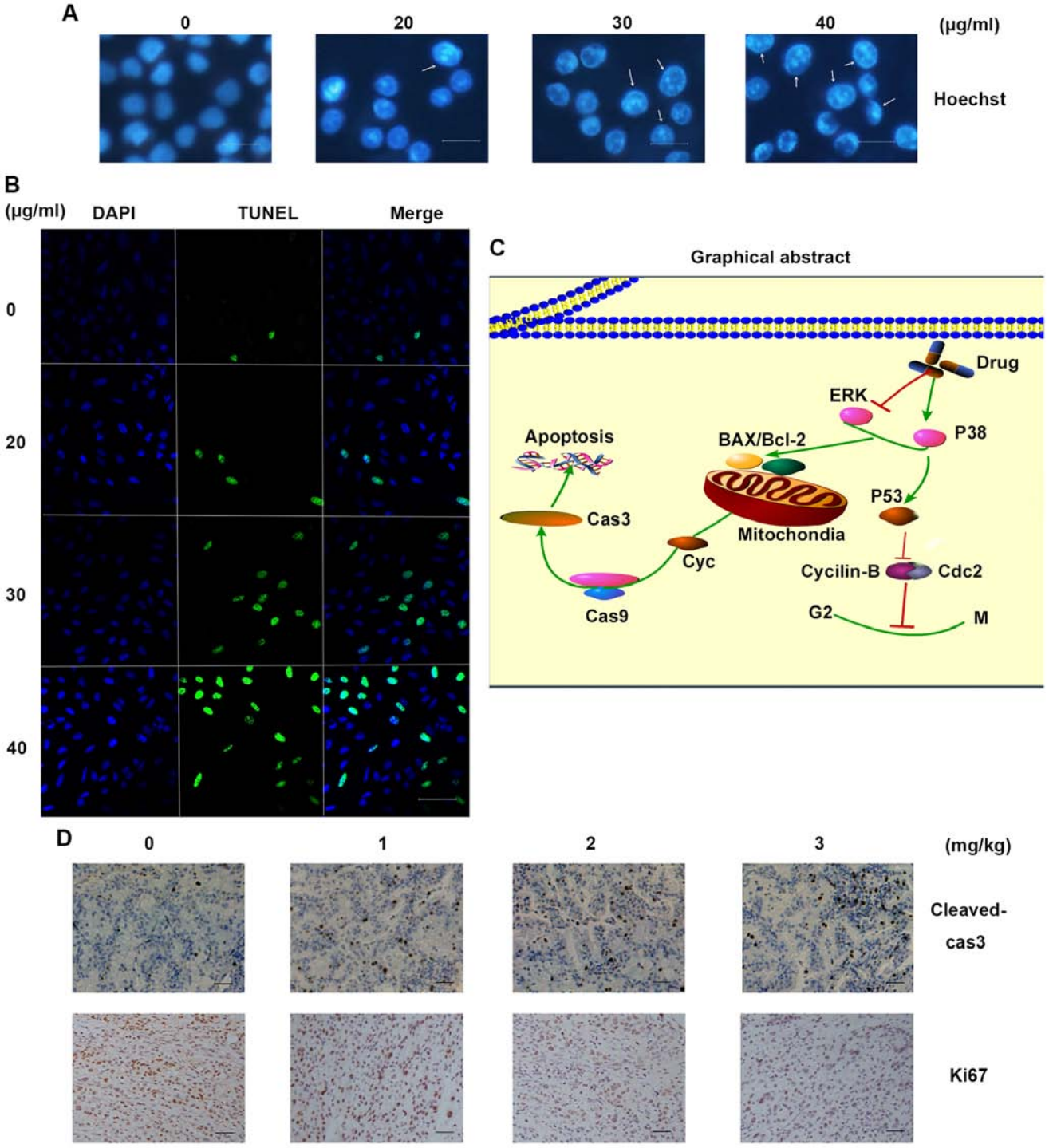


Figure 4. The visual effect of trifolirhizin on MKN45 cells and the underlying mechanism. Cells were exposed with increasing trifolirhizin for 48 h. (A) The Hoechst staining of MKN45 cells exposed with various doses of trifolirhizin for 48 h. Scale bar, 10 $\mu$m. (B) The TUNEL staining on glass cover of the MKN45 cells were imaged by immunofluorescence for DAPI (blue), TUNEL FITC (green) and their merging. Scale bar, 50 $\mu$m. (C) The graphical abstract of mechanism of trifolirhizin action on MKN45 cells. (D) IHC staining effect of trifolirhizin on the expression levels of cleaved-caspase-3 and Ki67 *in vivo*. Scale bar, 100 $\mu$m.

upgrade ratio of green/red fluorescence reflected that the MMP ($\Delta\Psi$m) in MKN45 after trifolirhizin treatment (20-40 $\mu$g/ml) was decreased.

The expression levels of the epidermal growth factor receptor (EGFR) signaling pathways and its downstream mitogen activated protein kinase (MAPK) signaling pathway were shared involving multiple anticancer agent molecular activities. The EGFR levels, containing RAS/RAF/MEK/ERK are downregulated with the increasing trifolirhizin, Fig. 4A indicates that trifolirhizin (20-40 $\mu$g/ml) triggered the increase of p38 and elicited no impact on p-JNK. Bcl-2 and Bax family members are the critical regulators in mitochondrial apoptosis pathways. Trifolirhizin leads to disorder of expression ratio of Bcl-2 and Bax. The induction of apoptosis

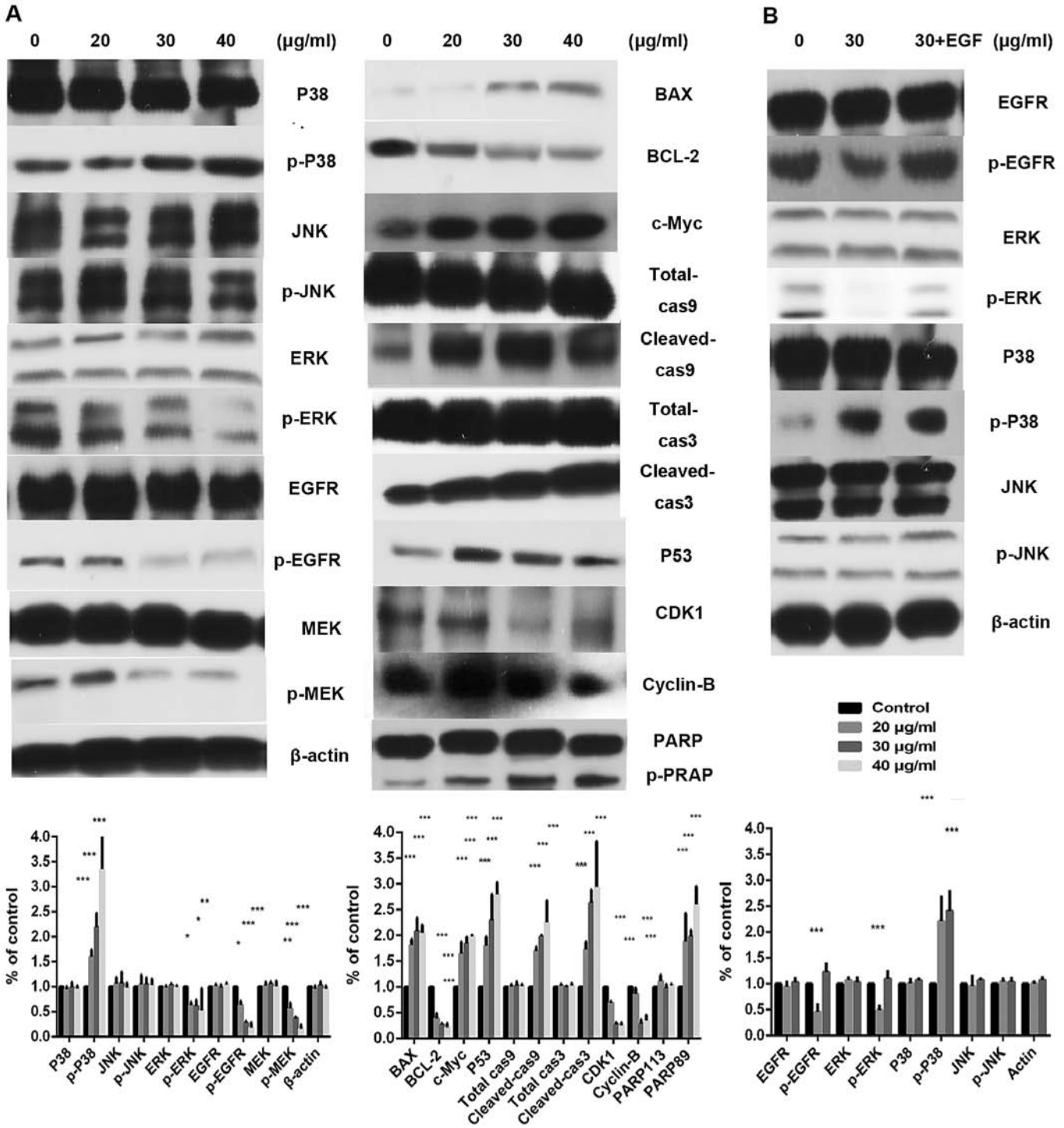


Figure 5. Mechanism of trifolirhizin induced apoptosis and cell cycle arrest in MKN45 cells. Cells were exposed for 48 h with increasing trifolirhizin (A) or combined with EGF (B). Protein levels were probed by western blot assay. Statistical differences between trifolirhizin treatment group vs. control group were considered significant at the levels of $^{*}P<0.05$, $^{**}P<0.01$ or $^{***}P<0.001$. Statistical differences between trifolirhizin treatment group vs. combination group were considered significant at the levels of $^{\#}P<0.05$, $^{\#\#}P<0.01$, $^{\#\#\#}P<0.001$.

by trifolirhizin was subsequently mediated through activities of c-Myc, caspase-9, and caspase-3.

*Trifolirhizin causes cell cycle arrest in human gastric cancer cells in vitro*. PI was employed to determine the cell cycle distribution under trifolirhizin exposure. Fig. 3 shows that trifolirhizin exposure (20-40 $\mu$g/ml) resulted in increasing accumulation in $G_2$/M phase in MKN45 cells. Furthermore, trifolirhizin exhibited impact on the cell cycle through regulation of cell cycle related proteins. There are an appreciable downregulation of cyclin B as well as Cdc2 in trifolirhizin treatment (20-40 $\mu$g/ml). The P53 protein, which is located upstream of cyclin complex and downstream of EGFR signaling pathways, is a key point between signaling pathway

Table I. The inhibitory effect of trifolirhizin on MKN45 implantation tumor growth in BALB/C-nu mice.

| Groups (mg/kg) | No. of animals survived | Body weights (g) | | Tumor weight (g) | Inhibition rate (%) |
|---|---|---|---|---|---|
| | | Start | End | | |
| Control | 6 | 20.35±0.68 | 24.6±0.98 | 1.42±0.42 | |
| 1 | 6 | 20.88±0.36 | 24.58±0.74 | 0.90±0.23[a] | 36.37 |
| 2 | 6 | 20.71±0.38 | 24.28±1.30 | 0.61±0.24[b] | 57.29 |
| 3 | 6 | 20.73±0.42 | 23.38±0.56 | 0.34±0.22[c] | 76.35 |

[a]P<0.05 vs. the vehicle control. [b]P<0.01 vs. the vehicle control. [c]P<0.001 vs. the vehicle control.

and cellular response in cell cycle arrest. Trifolirhizin treatment (20-40 $\mu$g/ml) elicited P53 activation (Fig. 5A).

*Anti-proliferation effect of trifolirhizin on MKN45 xenograft tumors*. Efficacy of trifolirhizin was also confirmed because there were few changes in the mouse body weight in the experiment (Fig. 1E). These results certified the relative safety of trifolirhizin *in vivo*. After 21 administration days, xenograft tumors treated with trifolirhizin (1-3 mg/kg) were smaller than control treated with saline (Table I and Fig. 1F). The significantly decreasing levels of Ki67-positive cells were found in the study, which hinted the anti-proliferation effect of trifolirhizin (1-3 mg/kg) *in vivo*. Cleaved-caspase-3 positive cells were increased which reflected the trifolirhizin apoptotic effect (Fig. 4D). These results also manifested the antitumor effects of trifolirhizin.

## Discussion

A previous published study indicated that trifolirhizin had cytotoxicity in several cancer cells (19). Despite the cytotoxicity on human cells by previous reports, the markedly higher $IC_{50}$ in our finding manifested the tissue specific effect of trifolirhizin on HEK293 (normal kidney cell) and L02 (normal liver cell). Therefore, trifolirhizin could be a potent safe anticancer candidate although the administration or the structure of trifolirhizin needs further efforts in future. In 2004, it was indicated that trifolirhizin induces apoptosis in HL-60 cells (23). However, the underlying apoptotic mechanism remains unclear. Thus, it was chosen as one candidate agent in our large scale natural anticancer compound screening for further efforts. The MKN45 cell is a typical gastric cancer cell commonly conducted as an antitumor model (24,25). Our assay indicated that trifolirhizin inhibited the proliferation of MKN45 gastric carcinoma cells in a time- and dose-dependent manner. Apoptosis hypothesis was further confirmed by flow cytometry data and visual contact under a microscope.

Many studies have indicated that EGFR-MAPK pathway has the ability to affect the Bcl-2 family (26). For instance, JNK can inactivate Bcl-2 while eliciting mitochondrial translocation of Bax (27). The Bcl-2 protein family is a crucial regulator of apoptosis (28). Bcl-2 protein family contain two main types of members: pro-apoptotic members Bax, anti-apoptotic members Bcl-2. The ratio of Bax/Bcl-2 leads to impaired apoptosis (29). In this study, imbalance in expression level of Bcl-2/Bax was clearly detected in the trifolirhizin treated MKN45 cells. MMP decreased significantly in trifolirhizin treated MKN45 cells. Loss of MMP contributes to the caspase pathway cascade (30). Caspases, a family of cysteine proteases, are important proteins in regulating the apoptotic response (31). Caspase-9 represents the intrinsic cascade pathway, while caspase-3 is the key executioner in apoptosis (32). Based on our western blot assay results, trifolirhizin induced the activation of caspase-9, caspase-3, and cleavage of PARP. Then apoptosis triggered cells to death. On the other hand, most cytotoxic agents usually inhibit cell proliferation via arresting the cycle in $G_1$/S or $G_2$/M phase (33,34). This arrest process is mediated with cyclin-dependent protein (Cdcs) with specific cyclin proteins. Trifolirhizin treatment leads to mediating accumulation in blocking of Cdc2 and inhibition of cyclin B resulting in a $G_2$/M phase arrest.

We used the EGF (100 ng/ml) to re-activate EGFR signal pathway for the mechanism validation (35). The apoptosis ratio in trifolirhizin (30 $\mu$g/ml) combined with EGF using flow cytometry assay was decreased compared with trifolirhizin (30 $\mu$g/ml, Fig. 2). The cell cycle distributions were also transformed (30 $\mu$g/ml, Fig. 3). The EGFR protein levels were upregulated in the combination group (30 $\mu$g/ml, Fig. 5B). The examination manifested that EGFR signaling pathway may be paramount in the effect of trifolirhizin on MKN45 cells.

In conclusion, trifolirhizin induced apoptosis in MKN45 cancer cells *in vitro* and *in vivo* mediated via EGFR-MAPK pathways. Trifolirhizin also arrest $G_2$/M cycle through impact on Cdc2/cyclin B complex (Fig. 4C). The results of this study implied that trifolirhizin may a feasible agent for anti-stomach tumor treatment, further scientific and therapeutic development should be established.

## Acknowledgements

This study was supported by State Administration of Traditional Chinese Medicine 'Twelfth Five Year Plan' Key Specialty (Chinese Medicine Geriatrics). The Shanghai Key Laboratory of Clinical Geriatric Medicine provided important technical support.

## References


1. Tang X, Hu G, Xu C, Ouyang K, Fang W, Huang W, Zhang J, Li F, Wang K, Qin X, *et al*: HZ08 reverse the aneuploidy-induced cisplatin-resistance in gastric cancer by modulating the p53 pathway. Eur J Pharmacol 720: 84-97, 2013.
2. Saika K and Sobue T: Cancer statistics in the world. Gan To Kagaku Ryoho 40: 2475-2480, 2013 (In Japanese).
3. Nomoto-Kojima N, Aoki S, Uchihashi K, Matsunobu A, Koike E, Ootani A, Yonemitsu N, Fujimoto K and Toda S: Interaction between adipose tissue stromal cells and gastric cancer cells in vitro. Cell Tissue Res 344: 287-298, 2011.
4. Fock KM: Review article: The epidemiology and prevention of gastric cancer. Aliment Pharmacol Ther 40: 250-260, 2014.
5. Hacker U and Lordick F: Current standards in the treatment of gastric cancer. Deutsche medizinische Wochenschrift 140: 1202-1205, 2015 (In German).
6. Safarzadeh E, Sandoghchian Shotorbani S and Baradaran B: Herbal medicine as inducers of apoptosis in cancer treatment. Adv Pharm Bull 4 (Suppl 1): 421-427, 2014.
7. Li HY, Zhang J, Sun LL, Li BH, Gao HL, Xie T, Zhang N and Ye ZM: Celastrol induces apoptosis and autophagy via the ROS/JNK signaling pathway in human osteosarcoma cells: An in vitro and in vivo study. Cell Death Dis 6: e1604, 2015.
8. Zhang HH, Kuang S, Wang Y, Sun XX, Gu Y, Hu LH and Yu Q: Bigelovin inhibits STAT3 signaling by inactivating JAK2 and induces apoptosis in human cancer cells. Acta Pharmacol Sin 36: 507-516, 2015.
9. Xin Y, Yin F, Qi S, Shen L, Xu Y, Luo L, Lan L and Yin Z: Parthenolide reverses doxorubicin resistance in human lung carcinoma A549 cells by attenuating NF-κB activation and HSP70 up-regulation. Toxicol Lett 221: 73-82, 2013.
10. Lin LL, Hsia CR, Hsu CL, Huang HC and Juan HF: Integrating transcriptomics and proteomics to show that tanshinone IIA suppresses cell growth by blocking glucose metabolism in gastric cancer cells. BMC Genomics 16: 41, 2015.
11. Ye B, Li J, Li Z, Yang J, Niu T and Wang S: Anti-tumor activity and relative mechanism of ethanolic extract of *Marsdenia tenacissima* (Asclepiadaceae) against human hematologic neoplasm in vitro and in vivo. J Ethnopharmacol 153: 258-267, 2014.
12. Kocevski D, Du M, Kan J, Jing C, Lačanin I and Pavlović H: Antifungal effect of *Allium tuberosum*, *Cinnamomum cassia*, and *Pogostemon cablin* essential oils and their components against population of *Aspergillus* species. J Food Sci 78: M731-M737, 2013.
13. Kim DW, Chi YS, Son KH, Chang HW, Kim JS, Kang SS and Kim HP: Effects of sophoraflavanone G, a prenylated flavonoid from *Sophora flavescens*, on cyclooxygenase-2 and in vivo inflammatory response. Arch Pharm Res 25: 329-335, 2002.
14. Hwang JS, Lee SA, Hong SS, Lee KS, Lee MK, Hwang BY and Ro JS: Monoamine oxidase inhibitory components from the roots of *Sophora flavescens*. Arch Pharm Res 28: 190-194, 2005.
15. Jung HJ, Kang SS, Hyun SK and Choi JS: In vitro free radical and ONOO- scavengers from *Sophora flavescens*. Arch Pharm Res 28: 534-540, 2005.
16. Fujise Y, Toda T and Itô S: Isolation of trifolirhizin from *Ononis spinosa* L. Chem Pharm Bull (Tokyo) 13: 93-95, 1965.
17. Zhang C, Ma Y, Gao HM, Liu XQ, Chen LM, Zhang QW, Wang ZM and Li AP: Non-alkaloid components from *Sophora flavescens*. Zhongguo Zhong Yao Za Zhi 38: 3520-3524, 2013 (In Chinese).
18. Abdel-Kader MS: Preliminary pharmacological study of the pterocarpans macckian and trifolirhizin isolated from the roots of *Ononis vaginalis*. Pak J Pharm Sci 23: 182-187, 2010.
19. Zhou H, Lutterodt H, Cheng Z and Yu LL: Anti-inflammatory and antiproliferative activities of trifolirhizin, a flavonoid from *Sophora flavescens* roots. J Agric Food Chem 57: 4580-4585, 2009.
20. Yang N, Liang B, Srivastava K, Zeng J, Zhan J, Brown L, Sampson H, Goldfarb J, Emala C and Li XM: The *Sophora flavescens* flavonoid compound trifolirhizin inhibits acetylcholine induced airway smooth muscle contraction. Phytochemistry 95: 259-267, 2013.
21. Hyun SK, Lee WH, Jeong DM, Kim Y and Choi JS: Inhibitory effects of kurarinol, kuraridinol, and trifolirhizin from *Sophora flavescens* on tyrosinase and melanin synthesis. Biol Pharm Bull 31: 154-158, 2008.
22. Yin T, Yang G, Ma Y, Xu B, Hu M, You M and Gao S: Developing an activity and absorption-based quality control platform for Chinese traditional medicine: Application to Zeng-Sheng-Ping (Antitumor B). J Ethnopharmacol 172: 195-201, 2015.
23. Aratanechemuge Y, Hibasami H, Katsuzaki H, Imai K and Komiya T: Induction of apoptosis by maackiain and trifolirhizin (maackiain glycoside) isolated from sanzukon (*Sophora Subprostrate Chen et T. Chen*) in human promyelotic leukemia HL-60 cells. Oncol Rep 12: 1183-1188, 2004.
24. Lindén SK, Driessen KM and McGuckin MA: Improved in vitro model systems for gastrointestinal infection by choice of cell line, pH, microaerobic conditions, and optimization of culture conditions. Helicobacter 12: 341-353, 2007.
25. Giard DJ, Aaronson SA, Todaro GJ, Arnstein P, Kersey JH, Dosik H and Parks WP: In vitro cultivation of human tumors: Establishment of cell lines derived from a series of solid tumors. J Natl Cancer Inst 51: 1417-1423, 1973.
26. Thomas S, Quinn BA, Das SK, Dash R, Emdad L, Dasgupta S, Wang XY, Dent P, Reed JC, Pellecchia M, *et al*: Targeting the Bcl-2 family for cancer therapy. Expert Opin Ther Targets 17: 61-75, 2013.
27. Yu H, Zhang T, Cai L, Qu Y, Hu S, Dong G, Guan R, Xu X and Xing L: Chamaejasmine induces apoptosis in human lung adenocarcinoma A549 cells through a Ros-mediated mitochondrial pathway. Molecules 16: 8165-8180, 2011.
28. Llambi F and Green DR: Apoptosis and oncogenesis: Give and take in the BCL-2 family. Curr Opin Genet Dev 21: 12-20, 2011.
29. Bah N, Maillet L, Ryan J, Dubreil S, Gautier F, Letai A, Juin P and Barillé-Nion S: Bcl-xL controls a switch between cell death modes during mitotic arrest. Cell Death Dis 5: e1291, 2014.
30. David R: Apoptosis: A lipid trigger of MOMP. Nat Rev Mol Cell Biol 13: 208-209, 2012.
31. Cohen GM: Caspases: The executioners of apoptosis. Biochem J 326: 1-16, 1997.
32. Brentnall M, Rodriguez-Menocal L, De Guevara RL, Cepero E and Boise LH: Caspase-9, caspase-3 and caspase-7 have distinct roles during intrinsic apoptosis. BMC Cell Biol 14: 32, 2013.
33. Carduner L, Picot CR, Leroy-Dudal J, Blay L, Kellouche S and Carreiras F: Cell cycle arrest or survival signaling through αv integrins, activation of PKC and ERK1/2 lead to anoikis resistance of ovarian cancer spheroids. Exp Cell Res 320: 329-342, 2014.
34. Romanov V, Whyard TC, Waltzer WC, Grollman AP and Rosenquist T: Aristolochic acid-induced apoptosis and G2 cell cycle arrest depends on ROS generation and MAP kinases activation. Arch Toxicol 89: 47-56, 2015.
35. Li L, Gao Y, Zhang L, Zeng J, He D and Sun Y: Silibinin inhibits cell growth and induces apoptosis by caspase activation, down-regulating survivin and blocking EGFR-ERK activation in renal cell carcinoma. Cancer Lett 272: 61-69, 2008.